LIMNOLOGY
and
OCEANOGRAPHY

ASLO

*Limnol. Oceanogr.* 60, 2015, 2090–2107

doi: 10.1002/lno.10156

# Size as the master trait in modeled copepod fecal pellet carbon flux

**Karen Stamieszkin,*[1] Andrew J. Pershing,[2] Nicholas R. Record,[3] Cynthia H. Pilskaln,[4] Hans G. Dam,[5] Leah R. Feinberg[6]**

[1]School of Marine Sciences, University of Maine, Orono, Maine
[2]Ecosystem Modeling Lab, Gulf of Maine Research Institute, Portland, Maine
[3]Ecosystem Modeling, Bigelow Laboratory for Ocean Sciences, Boothbay, Maine
[4]School for Marine Science and Technology, University of Massachusetts Dartmouth, New Bedford, Massachusetts
[5]Department of Marine Sciences, University of Connecticut, Groton, Connecticut
[6]Hatfield Marine Science Center, Oregon State University, Newport, Oregon

## *Abstract*

Zooplankton fecal pellet flux is a highly variable component of the biological carbon pump. While fecal pellets can comprise 0 to nearly 100% of particulate organic carbon collected in sediment traps, mechanisms for this variability remain poorly understood. Fecal pellet carbon flux is a complex function of several variables. We present a model that incorporates individual-scale metabolic processes to determine fecal pellet production rate, the relationship between body size and fecal pellet size, the relationship between fecal pellet size and sinking rate, and a function representing the breakdown of particles in the water column. When applied to copepod communities sampled by the continuous plankton recorder in the Gulf of Maine over 25 years, a seasonal pattern of fecal pellet carbon flux emerges. The interannual flux time series produced by the model reflects known oceanographic perturbations and shows how organism-scale processes can be scaled up to explain ecosystem level variability. We conclude that fecal pellet carbon flux in the Gulf of Maine is driven by copepod community size structure and copepod abundance, and that the fraction of fecal pellet carbon that reaches depth is a function of copepod size, rather than abundance. Changes in the physical environment which alter the size composition of the copepod community lead to variability in fecal pellet carbon flux. Our results indicate that incorporating size composition into biogeochemical models can more accurately constrain zooplankton-mediated carbon flux.

Relationships among marine primary production, oceanic carbon flux, global geochemical cycles, and climate are well established. In 1990, Martin published his famous "Iron Hypothesis," based on the premise that increased primary productivity could result in increased carbon flux to the seafloor, shifting Earth's climate toward a cooler regime (Martin 1990). However, this is an incomplete depiction of the processes at work in the world's oceans. Not all phytoplankton cells are equal with regard to flux, with particle size being the primary determinant of phytoplankton carbon flux to depth (Boyd and Newton 1999). Further, a complete understanding of variability in carbon flux must include top down grazing pressure in addition to primary productivity (Behrenfeld and Boss 2014). The set of processes that collectively result in organic matter sinking from the euphotic mixed layer to depth (i.e., the biological carbon pump) is not only an avenue of carbon sequestration in the deep ocean, but also connects the upper water column productivity to benthic productivity. Global patterns of biogeochemical cycling in the ocean reflect marine food web size structure (Legendre and Rassoulzadegan 1996), and these structures persist on a foundation of changing oceanographic and climatic conditions (Lutz et al. 2007).

Mechanisms underlying the relationship between ecosystem structure and biogeochemical cycling can be described on very broad (i.e., ecosystem) and very narrow (i.e., organism) scales; but scaling up from the latter to the former is a challenge. Mesozooplankton fecal pellet production and sinking is one highly variable component of the oceanic biological carbon pump (Turner 2002). This variability can be better understood by relating individual-scale biology to ecosystem-scale fecal pellet carbon (FPC) flux, or the amount of FPC reaching a target depth per unit time. Using metabolic theory and field observations, we built a size-based copepod FPC model that links Gulf of Maine copepod

Additional Supporting Information may be found in the online version of this article.

*Correspondence: karen.stamieszkin@maine.edu

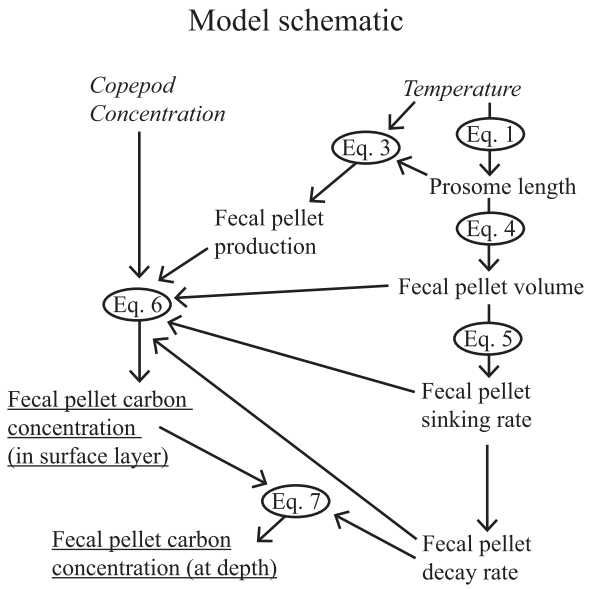


**Fig. 1.** Schematic diagram of the fecal pellet carbon model showing inputs (italicized), model variables (plain text) and outputs (underlined); the nodes represent the equations in the article.

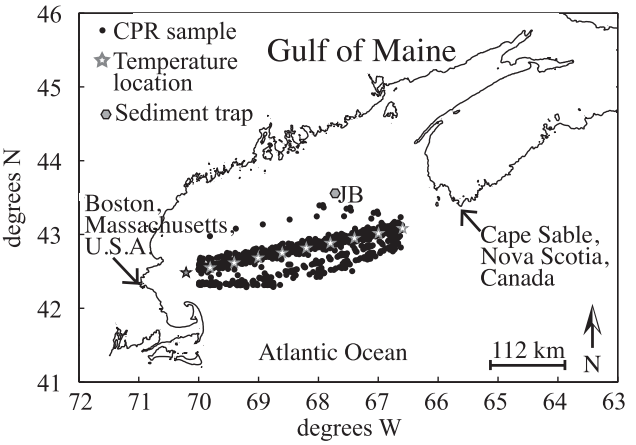


**Fig. 2.** The Gulf of Maine with locations of CPR zooplankton samples (black dots, January, 1988 to May, 2013), model temperature stations (stars), sediment trap location (JB = Jordan Basin, hexagon), and key geographic landmarks.

communities to seasonal and interannual patterns in estimated FPC concentration and flux.

We use copepod size as an organizing "master trait" (Litchman and Klausmeier 2008; Litchman et al. 2013) because it connects ecosystem structure with fecal pellet production and sinking rates, and therefore flux. The relative proportion of small to large mesozooplankton varies with latitude, temperature and nutrient regime (San Martin et al. 2006), and the sizes of individual copepods cumulatively result in varying community size spectra. Higher temperatures also result in smaller body size, within species (Record et al. 2012). Body size also determines fecal pellet size (reviewed in Mauchline 1998), and therefore sinking velocity, since settling speed is dependent on particle size (Guidi et al. 2008). By examining the computed cumulative fecal pellet production of copepod communities over different time scales, we provide a mechanistic explanation for seasonal and interannual FPC flux variability. We test the hypothesis that copepod community size composition and copepod abundance drive patterns in FPC reaching depth; we expect that higher proportions of larger copepods will result in higher relative FPC export.

## Methods

Our goal is to understand how changes in copepod community size structure and abundance can result in carbon export variability. We built a model that links copepod communities in a surface layer with fecal pellet flux to depth, in the Gulf of Maine. The model begins with copepod body size and builds to total fecal pellet carbon (FPC) produced in the surface layer, incorporating temperature-metabolism relationships. A size-based transport and decay function is used to estimate flux to a particular depth (Fig. 1). We applied this model to field observations from the Gulf of Maine Continuous Plankton Recorder (CPR) dataset (Fig. 2).

### Continuous plankton recorder copepod data

Continuous plankton recorders (CPRs) are sampling instruments, towed behind ships of opportunity, which collect and preserve plankton. The mesh size (270 $\mu$m) was chosen to give an accurate representation of the mesozooplankton and large phytoplankton, without clogging (Richardson et al. 2006). However, sampling with a 270 $\mu$m mesh under-samples smaller organisms, excluding fecal pellets produced by copepod species smaller than 270 $\mu$m from the model results. Comparison of absolute copepod abundance in the Gulf of Maine from the CPR time series and a Bongo net time series (1978–2006) show that the Bongo net is more efficient at capturing the most abundant copepods, possibly due to its lower tow speed. However, trends in interannual and seasonal abundance and composition are statistically similar in the two datasets for total zooplankton, and for the most abundant copepod species (Kane 2009). We applied our model to previously enumerated and taxonomically identified CPR samples ($n = 1961$). The samples were collected from January 1988 through May 2013, on a 452 km transect primarily between Boston, Massachusetts, U.S.A. and Cape Sable, Nova Scotia, Canada (Jossi et al. 2003) (Fig. 2). We excluded nearshore samples because zooplankton community composition tends to be different in coastal vs. offshore communities (Record et al. 2010). Each sample represents the organisms in approximately 100 $m^3$ of seawater, from approximately 7 m depth (Richardson et al. 2006). Only copepod data were included, as copepods make

**Table 1.** Summary of copepod species and stages included in this article; the "Percent of total" indicates the percent of all copepods in the CPR dataset represented by a given taxon; "Slope" ($m_i$) and "Intercept" ($b_i$) indicate the parameters used to calculate prosome length (*PL*) in the model, $PL = m_i(T) + b_i$, where *T* is temperature in °C; "Method" indicates how the *PL*-*T* relationship was determined: Literature = a published relationship was used; Calculated = relationship calculated fitting a line to min and max temperatures and lengths; Estimated = best estimate based on all available knowledge; Modeled = relationship back-calculated based on known relationship of a later stage and published growth rates. For full citations, see the Supporting Information 1: http://onlinelibrary.wiley.com/doi/10.1002/lno.10156/suppinfo.

| Species | Copepodid stage, sex | Percent of total | Slope | Intercept | Method | Literature used |
|---|---|---|---|---|---|---|
| *Calanus finmarchicus* | V | 10.2 | −33.1 | 2665 | Literature | Campbell et al. (2001) |
| *Calanus finmarchicus* | VIF | | −39.1 | 3073 | Literature | Campbell et al. (2001) |
| *Temora longicornis* | IV | 2 | −17.7 | 779.8 | Literature | Hirst et al. (1999) |
| *Temora longicornis* | VM | | −45.9 | 1333.1 | Literature | Hirst et al. (1999) |
| *Temora longicornis* | VIF | | −38.65 | 1265.8 | Literature | Deevey (1960) and Hirst et al. (1999) |
| *Metridia lucens* | V | 0.5 | −23.9 | 1594 | Calculated | McLaren et al. (1989), Batchelder and Williams (1995) and Hays et al. (1998) |
| *Metridia lucens* | VIF | | −32 | 2200 | Calculated | Batchelder and Williams (1995) and Hays et al. (1998) |
| *Centropages hamatus* | IV | 0.2 | −11.6 | 723 | Literature | Hirst et al. (1999) |
| *Centropages hamatus* | V | | −15.65 | 876.5 | Literature | Hirst et al. (1999) |
| *Centropages hamatus* | VIF | | −22.4 | 1162.5 | Literature | Hirst et al. (1999) |
| *Paraeuchaeta norvegica* | III | <0.1 | −28 | 1500 | Estimated | - |
| *Paraeuchaeta norvegica* | IV | | −31.9 | 2903.9 | Calculated | Tönnesson et al. (2006) |
| *Paraeuchaeta norvegica* | V | | −26.8 | 4366.2 | Calculated | Tönnesson et al. (2006) |
| *Paraeuchaeta norvegica* | VIF | | −31.6 | 5683.9 | Calculated | Tönnesson et al. (2006) |
| *Candacia armata* | V | <0.1 | −26.9 | 1309.4 | Modeled | Hirst et al. (1999), Richardson et al. (2001) and Ji et al. (2009) |
| *Candacia armata* | VIF | | −45.1 | 1830.8 | Calculated | Richardson et al. (2001) |
| *Pleuromamma robusta* | V | <0.1 | −11 | 1614 | Calculated | Park, unpubl. |
| *Pleuromamma robusta* | VIF | | −24 | 2253 | Calculated | Park, unpubl. |
| *Oithona* | IV | 6.3 | −2.7 | 213.8 | Modeled | Uye and Sano (1998) |
| *Oithona* | V | | −3.2 | 234 | Modeled | Uye and Sano (1998) |
| *Oithona* | VIF | | −2.2 | 344 | Literature | Uye and Sano (1998) |
| *Mecynocera clausi* | V | <0.1 | −10.1 | 726.2 | Modeled | Uye (1991), Ji et al. (2009) and Sun et al. (2012) |
| *Mecynocera clausi* | VIF | | −6 | 784 | Literature | Uye (1991), Sun et al. (2012) |
| *Metridia* | I | 0.7 | −7.2 | 497 | Calculated | McLaren et al. (1989) |
| *Metridia* | II | | −9.5 | 651 | Calculated | McLaren et al. (1989) |
| *Metridia* | III | | −12.4 | 853 | Calculated | McLaren et al. (1989) |
| *Metridia* | IV | | −15.9 | 1092 | Calculated | McLaren et al. (1989) |
| *Calanus* | I | 27.2 | −28.9 | 966 | Modeled | McLaren (1978) and Campbell et al. (2001) |
| *Calanus* | II | | −32.1 | 1147 | Modeled | McLaren (1978) and Campbell et al. (2001) |
| *Calanus* | III | 27.2 | −35.3 | 1432 | Modeled | McLaren (1978) and Campbell et al. (2001) |
| *Calanus* | IV | | −37.7 | 1838 | Modeled | |

**TABLE 1.** Continued

| Species | Copepodid stage, sex | Percent of total | Slope | Intercept | Method | Literature used |
|---|---|---|---|---|---|---|
| | | | | | | McLaren (1978) and Campbell et al. (2001) |
| *Acartia* | II | 0.8 | −4.6 | 491 | Literature | Durbin and Durbin (1978) |
| *Acartia* | III | | −4.8 | 567 | Literature | Durbin and Durbin (1978) |
| *Acartia* | IV | | −6.4 | 670.5 | Literature | Durbin and Durbin (1978) |
| *Acartia* | V | | −6 | 776 | Literature | Durbin and Durbin (1978) |
| *Acartia* | VIF | | −7.5 | 955 | Literature | Durbin and Durbin (1978) |
| *Paracalanus/ Pseudocalanus* | I | 10.4 | −17 | 515.9 | Modeled | Deevey (1960) and Ji et al. (2009) |
| *Paracalanus/ Pseudocalanus* | II | | −18.9 | 597.4 | Modeled | Deevey (1960) and Ji et al. (2009) |
| *Paracalanus/ Pseudocalanus* | III | | −20 | 691.4 | Modeled | Deevey (1960) and Ji et al. (2009) |
| *Paracalanus/ Pseudocalanus* | IV | | −23 | 799.7 | Modeled | Deevey (1960) and Ji et al. (2009) |
| *Paracalanus/Pseudocalanus* | V | | −25 | 924.3 | Modeled | Deevey (1960) and Ji et al. (2009) |
| *Pseudocalanus* | VIF | | −28.3 | 1212 | Literature | Deevey (1960) |
| *Pseudocalanus** | VIF | 8.2 | −28.3 | 1212 | Literature | Deevey (1960) |
| *Paracalanus* | VIF | 2.7 | −5.95 | 784 | Literature | Uye (1991) and Sun et al. (2012) |
| *Acartia danae* | II | <0.1 | −21.1 | 622.6 | Modeled | McLaren (1978); http://192.171.193.133/detail.php?sp=Acartia%20danae |
| *Acartia danae* | III | | −25.3 | 749.5 | Modeled | McLaren (1978); http://192.171.193.133/detail.php?sp=Acartia%20danae |
| *Acartia danae* | IV | | −31.7 | 946.1 | Modeled | McLaren (1978); http://192.171.193.133/detail.php?sp=Acartia%20danae |
| *Acartia danae* | V | | −44.6 | 1346.5 | Modeled | McLaren (1978); http://192.171.193.133/detail.php?sp=Acartia%20danae |
| *Acartia danae* | VIF | | −85 | 2615 | Calculated | McLaren (1978); http://192.171.193.133/detail.php?sp=Acartia%20danae |
| *Clausocalanus* | VIF | 0.1 | −25 | 924.3 | Modeled | Deevey (1960) and Ji et al. (2009) |
| *Centropages typicus* | IV | 12.9 | −9.2 | 1084.3 | Modeled | Deevey (1960), McLaren et al. (1989) and Liang et al. (1996) |
| *Centropages typicus* | V | | −10.7 | 1190.8 | Modeled | Deevey (1960), McLaren et al. (1989) and Liang et al. (1996) |
| *Centropages typicus* | VIF | 11.8 | −11.8 | 1266 | Literature | Deevey (1960) |
| *Nannocalanus minor* | V | <0.1 | −10 | 175 | Estimated | - |
| *Nannocalanus minor* | VIF | | −11 | 188 | Literature | Ashjian and Wishner (1993) |
| *Centropages bradyi* | VIF | <0.1 | −11.8 | 1266 | Literature | Deevey (1960) |
| *Candacia* | III | <0.1 | −16 | 949.9 | Modeled | Richardson et al. (2001), Ji et al. (2009) |
| *Candacia* | IV | | −19.8 | 1095.1 | Modeled | Richardson et al. (2001), Ji et al. (2009) |

**TABLE 1.** Continued

| Species | Copepodid stage, sex | Percent of total | Slope | Intercept | Method | Literature used |
|---|---|---|---|---|---|---|
| *Pleuromamma* | II | <0.1 | −4.6 | 661.6 | Calculated | Park, unpubl. |
| *Pleuromamma* | III | | −7.2 | 916.2 | Calculated | Park, unpubl. |
| *Pleuromamma* | IV | | −16 | 1198 | Calculated | Park, unpubl. |
| *Pleuromamma* | V | | −11 | 1614 | Calculated | Park, unpubl. |
| *Pleuromamma* | VIF | | −24 | 2253 | Calculated | Park, unpubl. |

**Pseudocalanus* spp. adult females were included as their own category, as well as in the *Paracalanus*/*Pseudocalanus* complex.

up the majority of the CPR zooplankton dataset (Kane 2009), and are the most numerous mesozooplankton group in the ocean (Mauchline 1998). This subset of the Gulf of Maine CPR time series was chosen for analysis because copepod taxonomic identification and enumeration were consistent throughout. In our model application, we used concentrations of 22 copepod taxa, which make up 94% of the organisms identified over the 25-yr period. Of the 6% excluded from analysis, 5.99% were of the CPR identification group, "copepod." We excluded these organisms due to their nonspecific identification. Of the 22 taxa included, 12 were identified to species, 9 to genus, and 1 to a grouping of two similarly sized genera (*Pseudocalanus/Paracalanus* spp.). The CPR dataset reports the abundances of each copepod taxon by combining copepodid stages. For example, *Calanus finmarchicus* abundance for each sample includes both stage C5 copepodids and adults (CVI), but is reported as one total abundance. Since our model is dependent on copepod size, which varies with life history stage, we divided each CPR abundance count into the number of stages included in that count. The most abundant taxa in the original CPR dataset are divided by older (CIV or CV–CVI) and younger (CI–CIII or CIV) developmental stages, reflecting some stage structure dynamics. Continuing the example, if a sample reported 500 *C. finmarchicus* $m^{-3}$, then we divided that by two to get 250 CV *C. finmarchicus* $m^{-3}$, and 250 CVI *C. finmarchicus* $m^{-3}$. Through this process, the original 22 stage/taxon combinations reported in the CPR dataset became 63 unique stage/taxon copepod groups (Table 1). More detailed stage information would yield more accurate FPC estimates.

### Temperature data

Monthly temperature estimates for the Gulf of Maine were extracted from the Northeast Coast Ocean Forecast System (NECOFS) model (http://fvcom.smast.umassd.edu/necofs/). NECOFS is a forecasting system that incorporates multiple submodels, including the Finite-Volume Coastal Ocean Model, configured for the Gulf of Maine, Georges Bank and New England Shelf (FVCOM-GOM). Hindcasts and comparative studies have shown that these models are accurate for temperature (Cowles et al. 2008). We therefore elected to use these data to provide a uniform source of depth-integrated temperatures for our entire CPR copepod time series.

We identified 10 locations that were centered along the CPR sampling track (Fig. 2) and extracted monthly temperature at each of those sites, from the NECOFS model. For each CPR copepod sample, we found the closest temperature location, and used a linear interpolation of time between the 2 months bounding the CPR sample date. We used an average of temperatures from the upper 30 m of the water column.

### Building the model

Our model has two key outputs: (1) FPC concentration in the surface layer, and (2) FPC concentration at a particular depth (underlined text in Fig. 1). From concentration at depth we also estimated FPC flux. Observed copepod community composition and concentration, and monthly temperature served as the model's foundation (italicized text in Fig. 1). With these data and known relationships between temperature, size, and metabolic rates, we derived a series of related variables necessary for estimating FPC concentration and flux (summarized in Table 2).

### Copepod lengths

The CPR dataset does not contain copepod lengths, which were critical to our model. Copepod prosome length is strongly related to the temperatures at which growth occurs (reviewed in Mauchline 1998). To reflect the impact of changing temperature on body size in our model, we needed a temperature-prosome length ($PL_i$, $\mu$m) relationship for each copepod stage/taxon ($i$) represented in the CPR dataset:

$$PL_i = m_i T + b_i \quad (1)$$

where $T$ is the temperature in °C, and $m_i$ and $b_i$ are parameters either from the literature or estimated. Published temperature-*PL* relationships were available for one third of the copepod stage/taxon groups, or 39.2% of all copepods in the dataset. We estimated the remaining temperature-*PL* relationships using one of two methods depending on the published information available. The first method is a "back-calculation" from older to earlier stages, and therefore requires a known temperature-*PL* relationship for an older copepodid stage, as well as parameters for a temperature-dependent development equation and a mass-specific growth

**Table 2.** Summary of input variables.

| Variable | Units | Minimum | Maximum | Mean | Median | Std. dev. |
|---|---|---|---|---|---|---|
| $PL_i$: prosome length | $\mu$m | 25.3 | $5.6 \times 10^3$ | $1.1 \times 10^3$ | $8.8 \times 10^2$ | 44.3 |
| $FPP_i$: fecal pellet production | Fecal pellets copepod$^{-1}$ h$^{-1}$ | 0.4 | 2.3 | 0.8 | 0.7 | 0.04 |
| $FPV_i$: fecal pellet volume | $\mu$m$^3$ | 20.2 | $2.3 \times 10^7$ | $9.3 \times 10^5$ | $1.9 \times 10^5$ | $1.6 \times 10^5$ |
| $SR_i$: fecal pellet sinking rate | m h$^{-1}$ | 0.1 | 8.8 | 2.2 | 1.9 | 0.7 |

equation. Copepod stage duration ($D_i$, days) is a function of temperature (Belehrádek 1935):

$$D_i = a(T+\alpha)^{\beta} \quad (2)$$

where $T$ is temperature in °C, $a$ and $\alpha$ are fitted parameters for each taxon ($i$). $\beta$ is −2.05 for Calanoid copepods (Corkett et al. 1986; Campbell et al. 2001; Record et al. 2012) and −2.6 for Cyclopoid copepods (Uye and Sano 1998) due to differences in their growth patterns. Instantaneous growth ($g$) was estimated using a temperature-dependent exponential model (Huntley and Lopez 1992). If both $D$ and $g$ are known, mass at a given stage can be calculated (Huntley and Lopez 1992; Record et al. 2012). We used a mass-specific inverse-growth equation to estimate the mass of earlier life stages ($M_{s\text{-}1}$, $\mu$m$^3$):

$$M_{s-1} = M_s e^{-gD_{s-1}} \quad (3)$$

where $g$ is the mass-specific growth rate, $D_{s\text{-}1}$ is the duration of the earlier stage, and $M_s$ is the mass of the older copepodid stage. The units are $\mu$m$^3$ because we used prosome length to the third power to estimate mass and vise versa; the two are consistently proportional to one another in copepods (Hirst 2012). This process was completed with the maximum, mean and minimum temperatures in our dataset, and from these three lengths, a linear model was applied and temperature-*PL* relationship determined (Eq. 1). Back-calculation was used to get temperature-*PL* relationships for approximately one third of the copepod stage/taxon groups, or 59.7% of the copepods in the dataset.

A second method was used when there was not enough published information to back-calculate a relationship. We fit a linear equation to minimum and maximum temperatures in our temperature dataset, and maximum and minimum copepod prosome lengths from field data in published papers, respectively. We used this method for 1.1% of the copepods. Finally, copepod species and stages for which no information was available were estimated based on the trajectory of later stages of that species, or length parameters of congeners; these stage/taxon groups made up < 0.0001% of the copepods in the dataset.

**Calculating fecal pellet carbon flux**

Metabolic functions, such as fecal pellet production, are scaled both to an organism's size, and to proximate environmental temperature (Brown et al. 2004). We calculated a fecal pellet production rate ($FPP_i$, fecal pellets copepod$^{-1}$ h$^{-1}$), the rate at which each copepod would produce fecal pellets. We used copepod size and local NECOFS temperature in an equation based on allometric and metabolic temperature dependence relationships (Brown et al. 2004):

$$\mathrm{FPP}_i = Ce^{-E/\mathrm{kT}}\mathrm{PL}_i^{\gamma} \quad (4)$$

where $C$ is a scaling constant. $E$ is activation energy (eV), $k$ is the Boltzmann constant ($8.62 \times 10^{-5}$ eV K$^{-1}$), $T$ is the temperature in K, $PL_i$ is the copepod prosome length (mm), and $\gamma$ is the mass scaling constant. Allometric scaling of metabolic rates usually refers to the mass of an organism, rather than length; therefore we estimated mass from length to the third power (Hirst 2012). Fecal pellet production rates also depend on prey availability (Besiktepe and Dam 2002). Therefore, parameters $E$ and $\gamma$ were estimated by fitting a model to observed fecal pellet production under a variety of food conditions, from limiting to nonlimiting (See the Supporting Information 1: http://onlinelibrary.wiley.com/doi/10.1002/lno.10156/suppinfo). Thus, estimated *FPP* assumes mean feeding conditions.

The volume of a copepod fecal pellet is directly related to the size of the pellet's producer (reviewed in Mauchline 1998). We estimated the volume of a single fecal pellet produced by each copepod ($FPV_i$, $\mu$m$^3$):

$$log_{10}FPV_i = \theta \log_{10}(PL_i) + \eta \quad (5)$$

where $PL_i$ is prosome length in mm, and $\theta$ and $\eta$ are parameters that we derived from fecal pellet dimensions and the prosome length of the copepod producing the fecal pellet. This was accomplished with a literature review (See the Supporting Information 1: http://onlinelibrary.wiley.com/doi/10.1002/lno.10156/suppinfo). We found a strong log-linear relationship between fecal pellet volume and pellet length ($n = 23$, $R^2 = 0.89$); therefore, when pellet volume was not available but pellet length was, this relationship was used to estimate volume.

The proportion of FPC produced near the sea surface that reaches a particular depth depends on the retention of fecal pellets in the water column (Feinberg and Dam 1998; Wexels Riser et al. 2002; Møller et al. 2011). Fecal pellets generally conform to Stokes Law, which indicates that sinking rate scales with pellet radius squared (Mauchline 1998). Smaller

fecal pellets, which therefore sink at disproportionately slow rates, are exposed to disaggregating processes for a longer period of time than larger, rapidly sinking pellets. We can use the sizes and numbers of the fecal pellets produced by a given copepod community, with an estimated retention rate as they sink through the water column, to estimate how much FPC reaches depth. From $FPV_i$, we estimated the sinking rate ($SR_i$, m $h^{-1}$) of each fecal pellet:

$$\log_{10} SR_i = \varphi \log_{10}(FPV_i) + \tau \quad (6)$$

where $\tau$ and $\varphi$ were calculated from compiled observations during experiments with different zooplankton feeding on different prey ($n = 806$, $R^2 = 0.60$) (Feinberg and Dam, unpubl., see the Supporting Information 1: http://onlinelibrary.wiley.com/doi/10.1002/lno.10156/suppinfo). $FPV_i$ ($\mu m^3$) was calculated as described above (Eq. 5).

Fecal pellet carbon concentration in the surface layer ($FPC_{sfc}$, mgC $m^{-3}$) is a function of the number of pellets produced ($FPP_i$), the volume of each pellet ($FPV_i$), the copepod concentration ($n_i$), and is adjusted for pellets sinking out of the surface layer where we assume FPC concentration to be constant. $FPC_{sfc}$ is one of the key model outputs, and is an estimate of total fecal pellet carbon mass produced by any given copepod community sampled by the CPR. A simple differential equation was used to represent the production of FPC in the surface layer, as well as fecal pellets sinking out (See the Supporting Information 2 for derivation: http://onlinelibrary.wiley.com/doi/10.1002/lno.10156/suppinfo); the following solution represents fecal pellet concentration in the surface layer:

$$FPC_{sfc} = \sum_i \left[ \frac{FPP_i \ \kappa \ FPV_i}{r + SR_i/h} n_i \right] \quad (7)$$

where $FPP_i$ (fecal pellets copepod$^{-1}$ $h^{-1}$) and $FPV_i$ ($\mu m^3$) are estimated as described above (Eqs. 4 and 5, respectively), and $n_i$ is observed copepod concentration of each stage/taxon category in the CPR dataset (copepods $m^{-3}$); $\kappa$ is a constant representing the nearly linear conversion from fecal pellet volume to FPC (Mauchline 1998). We used a conservative fecal pellet volume conversion of $25 \pm 5$ ngC per $FPV_i \times 10^6$ $\mu m^3$, derived from fecal pellets produced in the ocean by copepods feeding on an assemblage of natural prey (Urban-Rich et al. 1998). $SR_i$ is the fecal pellet sinking rate as a function of fecal pellet volume (Eq. 6); $h$ is the height of the surface layer for which the CPR sample is representative of copepod concentration. The CPR samples come from approximately 7 m; therefore we estimated that on average, the sample is representative of the top 14 m of the water column, with respect to copepod concentration. The fecal pellet remineralization rate ($r$) is the rate at which fecal pellets may be broken down and retained in the upper water column. In the ocean this rate changes in space and time (Wexels Riser et al. 2002; Møller et al. 2011), and the extent to which the decomposer community tracks production of detritus in the water column is unknown. We estimated $r$ for sinking fecal pellets by solving an exponential decay function representative of fecal pellet decay in the water column. We assumed that the mean ratio of FPC concentration at depth to FPC concentration in the surface layer ($FPC_{sfc}$), averaged over the entire time series, was constant. This scenario suggests that the detritivore community varies with the amount of material available, resulting in a constant decay rate (See the Supporting Information 2: http://onlinelibrary.wiley.com/doi/10.1002/lno.10156/suppinfo).

We then applied this decay function to the FPC concentration in the surface layer to estimate the amount of FPC reaching the depth of interest ($FPC_{d,}$ mgC $m^{-3}$):

$$FPC_d = \sum_i \left[ \frac{FPP_i \quad FPV_i}{r + \mathrm{SR}i/h} n_i \right] e^{(-r/\mathrm{SR}_i)z} \quad (8)$$

where $FPP_i$, $FPV_{i,}$ and $SR_i$ are calculated as described above, $n_i$ is copepod concentration from the CPR dataset, $\kappa$ is the fecal pellet volume to carbon conversion constant, $r$ is the remineralization rate, $h$ is the height of the surface layer, and $z$ is the depth of interest. Finally, we estimated FPC flux (mgC $m^{-2}$ $d^{-1}$) by multiplying $FPC_d$ by pellet sinking rate ($SR_i$), to give flux units mgC $m^{-2}$ $d^{-1}$.

**Error propagation and sensitivity analysis**

There is considerable uncertainty in the parameters that control the dynamics of the model. We estimated the impact of this uncertainty on the output variables. We also examined the sensitivity of the output to changes in the parameters.

We used a resampling method to propagate error through the calculations. Means and standard errors of the parameters were calculated during meta-analysis of published experimental data (Table 3). Normal distributions with those calculated means and error terms were assumed for all parameters. We calculated the model outputs (fecal pellet carbon concentration and flux) using parameter values that were randomly resampled from the normal distributions, with replacement ($n = 1760 \pm 20$). The variable values that we report (Table 2) are the averages and standard deviations of these recalculations. We did not assume a normal distribution of model outputs (FPC concentrations and flux) because the model variables interact nonlinearly during the calculation of FPC. We calculated the mean model outputs using the mean of each parameter (henceforth the "mean model"). This is the model that is most likely to occur, based on available data. The 95% confidence intervals, minima and maxima for the model outputs were calculated from all model runs ($n = 1760 \pm 20$), and represent the estimated lower and upper bounds for the true distribution of the model outputs.

**Table 3.** Summary of model parameters and the statistics associated with their fit to respective datasets (See the Supporting Information 1 for citations: http://onlinelibrary.wiley.com/doi/10.1002/lno.10156/suppinfo): fecal pellet production (*FPP*), fecal pellet volume (*FPV*), and fecal pellet sinking rate (*SR*).

| Variable | *n* | $R^2$ | *p* | Parameter | Mean | Standard error |
|---|---|---|---|---|---|---|
| *FPP* | 233 | 0.14 | <0.01 | $E$ | 0.28 | 0.005 |
| | | | | $\gamma$ | −0.24 | 0.005 |
| *FPV* | 188 | 0.43 | <0.01 | $\eta$ | 5.4 | 0.07 |
| | | | | $\theta$ | 2.58 | 0.22 |
| *SR* | 806 | 0.60 | <0.01 | $\tau$ | −0.03 | 0.06 |
| | | | | $\varphi$ | 0.32 | 0.01 |

We calculated the model outputs using three different remineralization rates ($r$ in Eqs. 7 and 8): 50%, 75%, and 95%. This showed the effect of fecal pellet retention rate as the pellets fall through the water column. We also tested the sensitivity of our model to the variability of each input variable by calculating fecal pellet carbon flux seven times; each time we held the parameters associated with zero, one or two variables constant (i.e., none, *FPV*, *FPP*, *SR*, *FPV* + *FPP*, *FPV* + *SR*, and *FPP* + *SR*). This test allowed us to see whether one input variable disproportionately contributed to the model output variability.

### Annual climatology

We calculated a one-year climatology of FPC concentration over an average annual cycle. A biweekly moving average of FPC concentration in the surface layer ($FPC_{sfc}$) and at the mean depth of the Gulf of Maine (139 m, $FPC_d$) was determined for each year, from 1988 to 2012; the year 2013 was excluded because data were only available through May that year. The corresponding biweekly means from each year were averaged together to provide the mean annual climatology of FPC concentration. We chose to use a moving average to show the seasonal trends over the course of a year, and to smooth the high spatial heterogeneity typical of zooplankton distributions over the Gulf of Maine. We also calculated the absolute and relative contributions of copepods from five size ranges, to the FPC reaching the seafloor; this showed how copepod size affects $FPC_d$ over an annual cycle in the Gulf of Maine.

We calculated a FPC export efficiency term (henceforth "FPC flux efficiency"), representing the fraction of FPC produced at the surface that reaches the target depth, to explore the relative importance of copepod concentration and body size. It was calculated as the ratio of $FPC_d$ to $FPC_{sfc}$. We assumed that 75% of the pellets produced at the surface were remineralized in the water column before reaching the 139 m depth horizon. Fecal pellet retention in the Barents Sea (i.e., the proportion produced reaching a target depth) has been reported as 40% at an ice edge to 96% in the Atlantic sector (Wexels Riser et al. 2002). We used this range as a guideline because fecal pellet retention has not been measured in the Gulf of Maine. Thus, a 75% retention rate represents moderate retention. Mean copepod lengths and mean community concentrations were also calculated to compare to the model outputs.

### Comparison of model results to field data

Direct validation of this model would require long-term sediment trap samples from under the Gulf of Maine CPR transect, analyzed for their copepod fecal pellet content; however, such data do not presently exist. We compared our FPC flux estimates to data from Gulf of Maine sediment trap samples. The traps were deployed at 150 m in Jordan Basin, Gulf of Maine (43° 29.9 N; 067° 50.3 W) from 19 September 1995 to 24 April 1997, and 05 April 2005 to 14 April 2006 (Fig. 2), and were part of the National Atmospheric and Oceanic Administration's (NOAA) Regional Marine Research Program (RMRP) and the Ecology and Oceanography of Harmful Algal Blooms (ECOHAB) Program (methods described in Pilskaln et al. 2014). We compared the relative difference between modeled annual FPC flux, and the mean calculated POC flux measured by the 150 m time-series traps in 1995–1997 ($n = 39$ samples) and 2005–2006 ($n = 26$ samples). The discrepancy between the location of the sediment traps and the CPR transect limits our ability to make a direct comparison. However, we expect that any correspondence between the two would occur at long time scales; thus we focused on comparing the interannual signals. With this comparison we tested whether changes in the modeled FPC values reflect relative interannual changes in POC flux documented by sediment traps.

## Results

### Model parameterization

We constructed our model with several submodels based on allometric scaling and metabolic theory. Each submodel was a step toward calculating the amount of fecal pellet carbon (FPC) that a copepod produces, starting with copepod size, and ending with FPC concentration at depth and flux (Fig. 1). We parameterized the submodels by fitting curves to published data (See the Supporting Information 1: http://onlinelibrary.wiley.com/doi/10.1002/lno.10156/suppinfo), and resampled

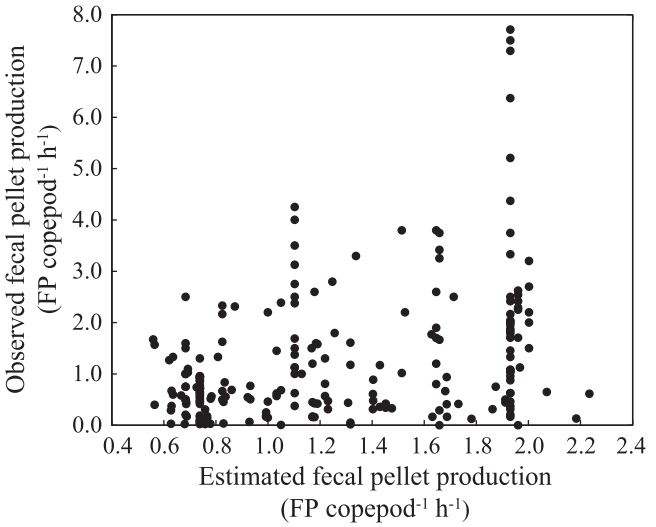


**Fig. 3.** Estimated fecal pellet production (*FPP*) vs. observed *FPP* ($n = 233$, $r = 0.37$, $p < 0.01$); the *FPP* model assumes mass-dependent scaling of metabolic rates, and an Arrehnius-type temperature function.

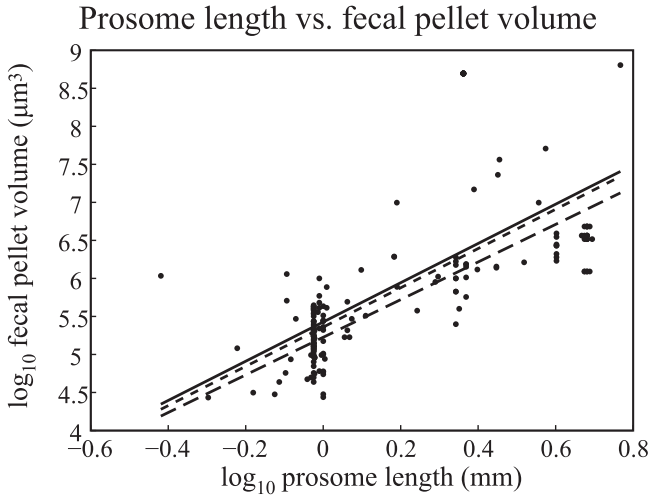


**Fig. 4.** Prosome length (*PL*) vs. fecal pellet volume (*FPV*), on a log-log scale; dots represent data points used in this article's analysis of the *PL-FPV* relationship, with the solid line indicating the line of best fit ($R^2 = 0.43$, $p < 0.01$). The dashed lines represent the same relationship determined in previous similar studies: small-dashed from Uye and Kaname (1994), large-dashed from Mauchline (1998).

parameter distributions to estimate a distribution of modeled FPC outputs ($n = 1760 \pm 20$).

Each copepod species/stage used in this analysis has a unique temperature-prosome length relationship based on the experimental literature or our modeling work described above (Table 1). Fecal pellet production rates were modeled from relationships in the literature (See the Supporting Information 1: http://onlinelibrary.wiley.com/doi/10.1002/lno.10156/suppinfo) between fecal pellet production, prosome length and temperature ($n = 235$, $r = 0.37$, $p < 0.01$) (Fig. 3). Estimated fecal pellet production rates are lower than published values, but not unreasonable, making the model estimates of FPC conservative (Table 3; See the Supporting Information 1: http://onlinelibrary.wiley.com/doi/10.1002/lno.10156/suppinfo). The literature review of fecal pellet volume and their producers' prosome lengths yields a log-linear relationship ($n = 188$, $R^2 = 0.43$, $p < 0.01$) (Fig. 4; Table 3) as seen in other studies (Uye and Kaname 1994; Mauchline 1998). Fecal pellet sinking rate is also a log-linear function of fecal pellet volume (Table 3, Feinberg and Dam, unpubl.).

### Annual cycle of fecal pellet carbon concentration and flux

The modeled mean annual cycle of FPC concentration in the surface layer ($FPC_{sfc}$) shows two distinct peaks: one in the first half of June and a secondary peak in the first half of October (Fig. 5a). The FPC concentration at 139 m ($FPC_d$) shows the same primary peak, but a lesser secondary peak (Fig. 5b). The model outputs are not normally distributed, but skewed toward lower FPC values. The parameters can be seen as scaling terms, which determine whether the model output is relatively high or low, but for any given model output, FPC will be scaled the same way. In other words, the position of the output within the model's distribution is predetermined, and the FPC estimates for that model run will be scaled the same way. In this case, it is possible to have FPC concentrations more than three times that predicted by the mean model (Fig. 5).

We hypothesized that higher numbers of larger copepods would result in higher FPC export. When we divide $FPC_{sfc}$ and $FPC_d$ into the contributions of five copepod size bins, the importance of smaller vs. larger copepods is apparent, as is the annual cycle of copepod size in the Gulf of Maine (Fig. 6). For an average copepod community during each month, the smaller copepod size classes ($< 1500$ $\mu$m) contribute more FPC to $FPC_{sfc}$ (Fig. 6a,b) than to $FPC_d$ (Fig. 6c,d); and the percent of FPC contributed by the larger copepods is always higher at depth than in the surface layer, for each month. The smallest copepods ($< 500$ $\mu$m) make 1.0–3.9% of $FPC_{sfc}$ (Fig. 6a,b), but none of this FPC reaches depth (Fig. 6c,d). The copepods from the largest size bin ($\geq 4000$ $\mu$m) contribute a maximum of 2.4% $FPC_{sfc}$ in July, but up to 4.3% of $FPC_d$ in the same month. The dominant size bin switches between June and August; earlier in the year, the 1500–3999 $\mu$m group contributes the majority of FPC both to the surface layer and depth. In the latter half of the year, FPC from the 1000–1499 $\mu$m group dominates (Fig. 6).

We expect a relationship between model inputs (e.g., concentration and length) and the outputs (e.g., FPC), but because the model is nonlinear these comparisons can elucidate which factors are driving changes in estimated FPC concentration and flux throughout the annual cycle. When we

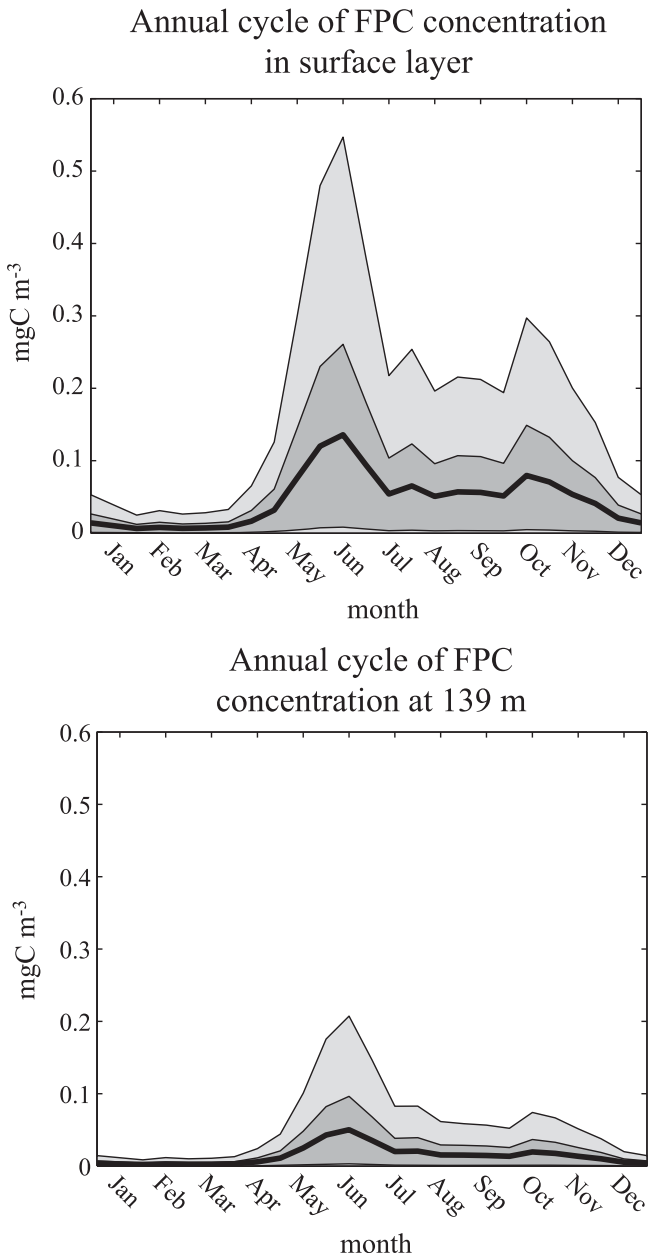


**Fig. 5.** Model results: (a) annual climatology of fecal pellet carbon concentration in the surface layer ($FPC_{sfc}$) and (b) fecal pellet carbon concentration at 139 m ($FPC_d$), estimated by the model; the black lines represent the mean model, or the model most likely to occur. Dark gray represents the 95% confidence interval, and light gray represents the minimum and maximum model outputs. Values are represented as a biweekly moving average to emphasize trends, and a 75% retention rate was used.

directly compare copepod concentration to FPC concentrations, we see that the annual cycles of $FPC_{sfc}$ and $FPC_d$ are both tightly coupled to copepod concentration in the surface layer ($FPC_{sfc}$: $R^2 = 0.96$, $p < 0.01$; $FPC_d$: $R^2 = 0.83$, $p < 0.01$). However, at the start of July, there is a change in how copepod concentration affects the magnitude of FPC export (Fig. 7a); the relationship between the two over the year is nonlinear. We found that a change in copepod size composition explains this shift. The mean copepod length begins to drop in July, as does FPC flux efficiency (ratio of $FPC_d$ to $FPC_{sfc}$); FPC flux efficiency is more closely associated with mean copepod prosome length ($R^2 = 0.72$, $p < 0.01$), than copepod concentration ($R^2 = 0.02$, $p = 0.49$) throughout the year (Fig. 7b). This annual pattern is also reflected in the mid-summer shift from larger to smaller copepod size class contributing most to FPC (Fig. 6).

### Model sensitivity

The model outputs show a high level of sensitivity to remineralization or retention rate ($r$) of fecal pellets as they sink through the water column (Fig. 8). We also tested the model sensitivity to each variable and combination of variables by holding the parameters associated with each variable constant, and plotting the width of the 95% confidence interval for FPC flux (Fig. 9). Holding the sinking rate parameters constant had the greatest impact on the model outputs, followed by fecal pellet production rate.

### Interannual variability in fecal pellet carbon concentration and flux

$FPC_{sfc}$, $FPC_d$ and FPC flux all show significant interannual variability, but no significant trends over the study period (Fig. 10). FPC flux (Fig. 10c) mirrors the patterns in $FPC_{sfc}$ and $FPC_d$ (Fig. 10a,b, respectively) with a few exceptions, most notably in 1988 and 1989 when $FPC_{sfc}$ and $FPC_d$ are relatively low, but flux is relatively high. During these two years, the mean copepod prosome length in the Gulf of Maine was up to two times higher than in any other year. All FPC variables are lowest in 1998 as is the variability around the mean model; 2011 and 2012 follow as the next lowest years in FPC flux (Fig. 10). The two years of available sediment trap data from Jordan Basin (19 September 1995 to 24 April 1997, and 05 April 2005 to 14 April 2006) corroborate the relative difference between the modeled FPC variables from those two years. The mean 150 m POC flux was 6.8 mg $m^{-2}$ $d^{-1}$ and 4.2 mg $m^{-2}$ $d^{-1}$ during the earlier and later periods, respectively; all FPC variables reflect this relative difference (Fig. 10).

## Discussion

Many processes mediate the amount of organic carbon that falls to the seafloor, or past the 1000 m "sequestration depth" in the ocean, where it is considered decoupled from the ocean-atmosphere system (Primeau 2005; Passow and Carlson 2012). The sum of processes that augment flux, such as aggregation and ballasting, and those that decrease it, such as decomposition and remineralization, result in a variable biological carbon pump. Sinking zooplankton fecal pellets represent a highly variable portion of the biological carbon pump; the particulate organic carbon found in

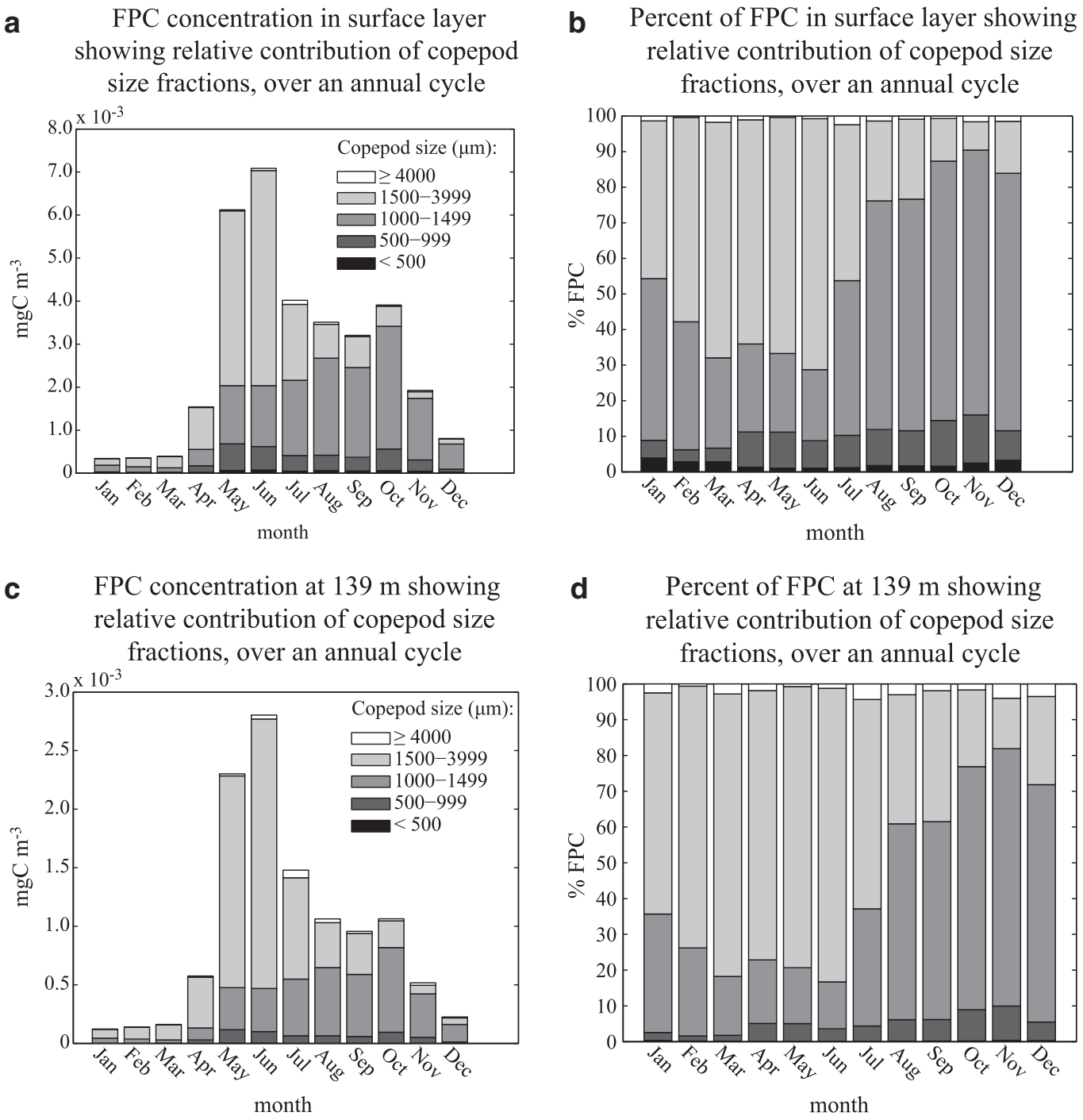


**Fig. 6.** Mean fecal pellet carbon concentrations and percent compositions, broken into the contribution of five copepod size-classes represented by shades of gray (< 500 $\mu$m black; 500–999 $\mu$m dark gray; 1000–1499 $\mu$m medium gray; 1500–3999 $\mu$m light gray; and ≥ 4000 $\mu$m white) for each month; (a) annual climatology of fecal pellet carbon concentration in the surface layer ($FPC_{sfc}$), (b) percent composition of $FPC_{sfc}$, (c) annual climatology of fecal pellet carbon concentration at 139 m ($FPC_d$), (d) percent composition of $FPC_d$. A 75% retention rate was used for all.

sediment traps can be composed of 0–100% zooplankton fecal pellets (reviewed in Turner 2002). We suggest that FPC flux variability can be explained in the Gulf of Maine using copepod body size as a master trait.

In our model, the annual cycle of fecal pellet flux efficiency, or the fraction of fecal pellet carbon (FPC) produced that reaches a target depth, is tightly coupled with mean copepod body size. While metabolic theory indicates that smaller

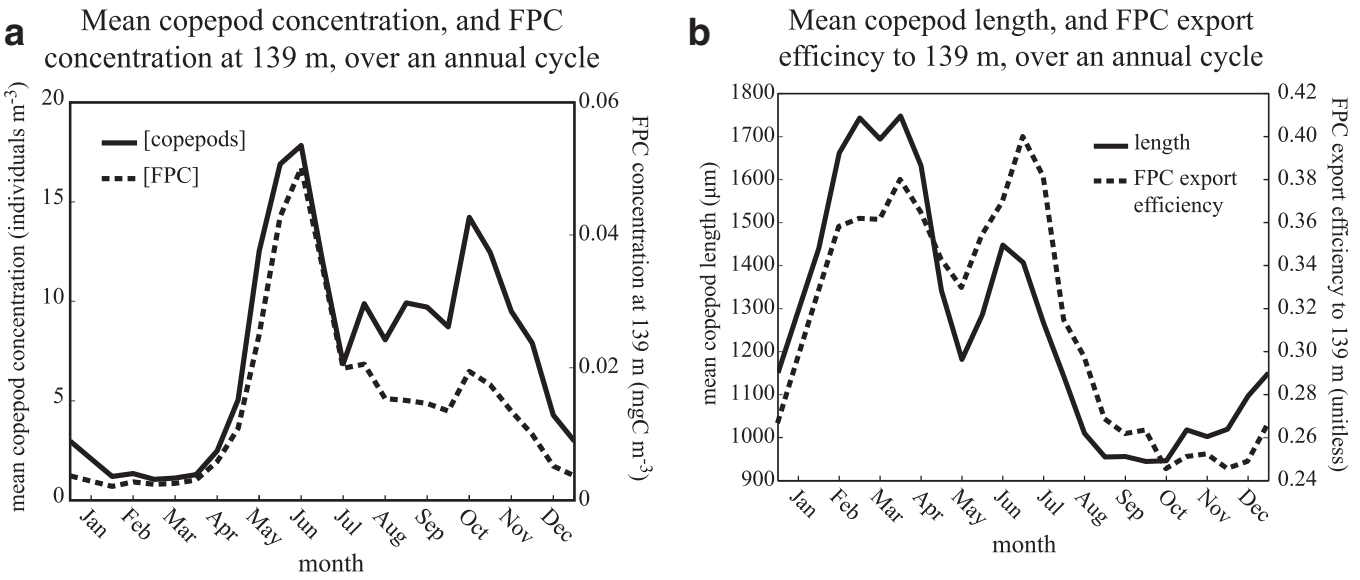


**Fig. 7.** (a) Annual climatology of copepod concentration represented by the solid line, and annual climatology of fecal pellet carbon concentration at 139 m ($FPC_d$) represented by the dashed line; (b) annual climatology of copepod community mean length represented by the solid line, and annual climatology of fecal pellet carbon (FPC) flux efficiency (ratio of FPC concentration at 139 m to concentration in the surface layer) represented by the dashed line. All climatologies are represented as biweekly moving averages; retention of fecal pellets in the water column is assumed to be 75%; data from 1988 to 2012 were used.

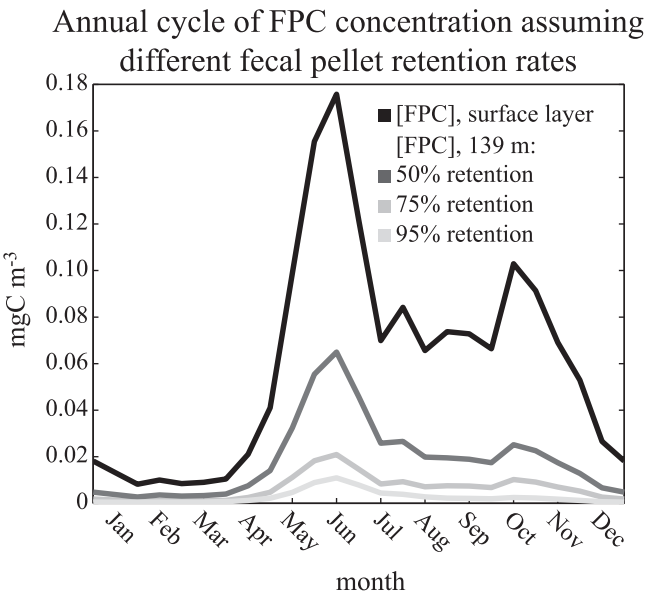


**Fig. 8.** Fecal pellet carbon concentration in the surface layer ($FPC_{sfc}$) represented by the black line; fecal pellet carbon concentration at 139 m ($FPC_d$) assuming 50% (dark gray), 75% (medium gray) and 95% (light gray) retention of fecal pellets in the water column. Data from 1988 to 2012 were used.

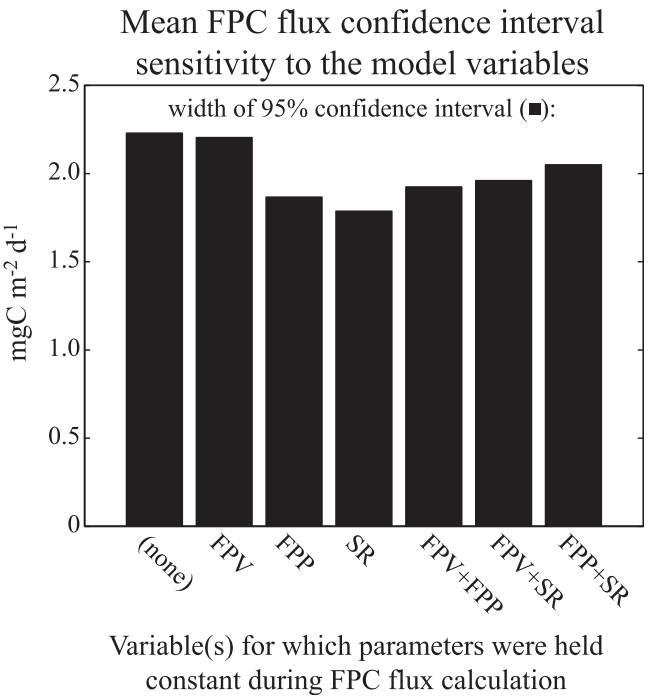


**Fig. 9.** 95% confidence interval widths for the mean fecal pellet carbon (FPC) flux, as the model is run holding the parameters for none, one, or two variables constant. A 75% retention rate was used.

copepods produce more fecal pellets per time than larger copepods due to relatively high metabolisms (Brown et al. 2004), larger pellets sink disproportionately faster than small pellets (Guidi et al. 2008; Feinberg and Dam, unpubl.), and pellet size is directly related to copepod size. Since pellet size affects not only carbon content per pellet (Urban-Rich et al. 1998), but also sinking rate, it reduces the amount of time that a pellet is exposed to coprophagy, coprohexy and bacterial degradation

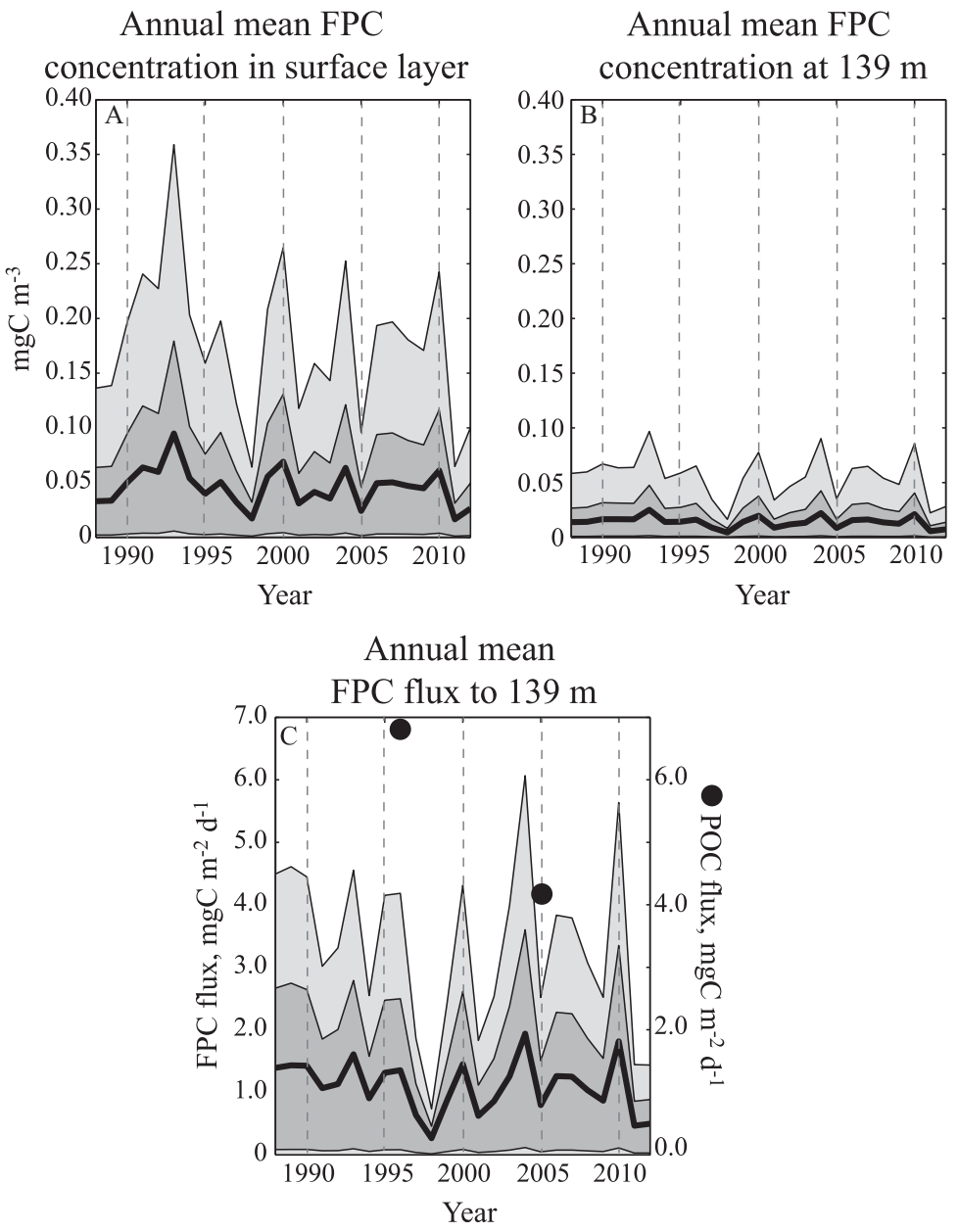


**Fig. 10.** Modeled time series of annual mean (a) copepod fecal pellet carbon (FPC) concentration in the surface layer ($FPC_{sfc}$), (b) FPC concentration at 139 m ($FPC_d$), and (c) FPC flux, as well as annual average particulate organic carbon (POC) flux measured in sediment traps (black dots); the black lines represent the mean model; dark gray represents the 95% confidence intervals, and light gray represents the minimum and maximum models. A 75% retention rate was used for all.

(Turner 2002) in the water column. Therefore, copepod body size has a compounding effect on FPC flux.

The extent to which fecal pellets are broken down as they sink through the water column is clearly important, demonstrated by the sensitivity of estimated FPC concentration at depth to percent remineralization (Fig. 8). This rate of retention is the least constrained of our model inputs. Bacterial degradation of pellets is a complex function of temperature (Honjo and Roman 1978) and grazer diet (Thor et al. 2003); it can vary spatially in the horizontal and vertical directions (Alonso-Sáez et al. 2007; Baltar et al. 2007), as well as temporally (Turley et al. 1995). Further, copepods themselves are known to break apart and consume fecal pellets (Iversen and Poulsen 2007). Models of biogenic carbon flux such as this would greatly benefit from a more detailed understanding of the mechanisms behind POC retention as particles sink through the water column.

The interplay between copepod abundance and size throughout the year affects the amount of FPC reaching depth. With size held constant, higher copepod abundance implies that more fecal pellets are produced and may sink. However, copepod size varies seasonally and is decoupled from abundance. The annual cycle of FPC flux efficiency ($FPC_d$: $FPC_{sfc}$) compared with that of copepod size highlights the importance of size with regard to the fraction of FPC in the surface layer that reaches depth (Fig. 7b). Efficiency is high in the winter because the community is dominated by large species, but actual FPC flux is low because copepod abundance is low. Maximum FPC flux and efficiency occur in the late spring and early summer because mean copepod size and abundance both increase. Gulf of Maine time-series trap data from a number of offshore sites and time periods spanning 1995–2010 document late spring/summer total mass flux and POC flux peaks to which fecal pellets contribute along with algal aggregates (Pilskaln et al. 2014; Pilskaln, unpubl.). In the fall a secondary peak in copepod abundance coincides with the lowest FPC flux efficiency values throughout the year (Fig. 7). This is due to relatively small mean body size, resulting in smaller, slower-sinking pellets that are degraded faster than large pellets. We therefore observe a lower modeled efficiency of pellets reaching the target depth, compared with the spring/summer period.

The model results suggesting that small copepods are less important to fecal pellet flux than large copepods, even when highly abundant, are consistent with findings from the field elsewhere. A northern Norwegian study found that relatively large fecal pellets from adult individuals of the copepod *Calanus finmarchicus* contribute disproportionately to flux compared with the much smaller and more abundant *Oithona similis* (Wexels Riser et al. 2010). During the same field campaign, the summer copepod community was dominated by small copepod species and stages, resulting in high fecal pellet abundance in the water column (Pasternak et al. 2000), but low fecal pellet flux (Wexels Riser et al. 2010). The agreement of these results with the modeled results from the Gulf of Maine supports the mechanistic framework that our model provides. Patterns of copepod fecal pellet flux can be explained using trait-based predictions of individual-scale biology.

*Calanus finmarchicus* is the only large-bodied, highly abundant copepod in the Gulf of Maine. The primary peak in FPC flux during late spring/early summer is driven by *C. finmarchicus* abundance. The diversity in the Gulf of Maine copepod community can be reduced to body size to explain variability in FPC flux; however, *C. finmarchicus* dynamics are a unique and primary factor in interannual differences in flux, due to the species' relative large size and high abundance. Advection is an important mode of *C. finmarchicus* transport into and around the Gulf of Maine (Lynch et al. 1998; Greene and Pershing 2000). Mode shifts in the North Atlantic Oscillation, a decadal-scale climate oscillation, can change Northwest Atlantic and Gulf of Maine circulation, impacting *C. finmarchicus* abundance (Greene and Pershing 2000; Conversi et al. 2001). Temperature and chlorophyll concentrations can also affect *C. finmarchicus* abundance by impacting the body size and egg production of females (Melle et al. 2014). *C. finmarchicus* abundance is declining in the North Sea (Beaugrand et al. 2009), and its range is projected to shift north, excluding the Gulf of Maine (Reygondeau and Beaugrand 2011). Although long-term sediment trap data are lacking for direct model validation, there is a correlation between the annual growth of a long-lived benthic clam from the Gulf of Maine, and Gulf of Maine *C. finmarchicus* abundance measured by the CPR (Wanamaker et al. 2009). The clam can be seen as a living sediment trap, with growth reflecting prey availability near the seafloor. This relationship is consistent with variations in *C. finmarchicus* leading to changes in the flux of organic material to the benthos. Based on our model results, a decrease in *C. finmarchicus* in the Gulf of Maine would likely lead to a decrease in carbon export and delivery to the benthos.

The interannual changes in our modeled FPC concentration at depth (mgC $m^{-3}$), as well as flux (mgC $m^{-2}$ $d^{-1}$) are broadly consistent with the interannual variability in available sediment trap data (Pilskaln, unpubl.). This comparison indicates that our model may accurately reflect relative changes in FPC flux. The magnitude of FPC flux estimated by the model fits well within the range of reported FPC fluxes in the literature from different systems, and within the POC estimates from the sediment traps. FPC fluxes measured at similar depths around the world range from less than 1 mgC $m^{-2}$ $d^{-1}$ (Goldthwait and Steinberg 2008; Gleiber et al. 2012) to 135 mgC $m^{-2}$ $d^{-1}$ (Stukel et al. 2013).

Sinking rate was the variable that had the most impact on the model's mean 95% confidence interval width, followed by fecal pellet production rate (Fig. 9). Experimental work aimed at fine-tuning the parameterization of these variables would improve our model. As discussed above, fecal pellet remineralization rate also has a significant impact on our model outputs. An improved fecal pellet decay function that varies with environmental parameters such as temperature, depth, and time of year would improve the model's estimate of flux. The model depends heavily on the conversion from fecal pellet volume to fecal pellet carbon. This conversion is known to change seasonally and with prey type (Urban-Rich et al. 1998). Improvement of the fecal pellet volume to carbon conversion would improve this model as well.

Our model shows the potential for changes in zooplankton composition and concentration to drastically alter the FPC flux. This variability underscores the complexity of ground-truthing models of FPC flux. The ocean is a patchy environment and zooplankton patches persist over varying spatial and temporal scales (Folt and Burns 1999). Zooplankton fecal pellet flux events are therefore episodic and hard to document. Our novel approach to modeling fecal pellet flux,

using Gulf of Maine CPR zooplankton abundances, aims to reflect the patchy nature of zooplankton and discontinuous nature of fecal pellet flux over time and space. Further, by incorporating the effects of size on metabolism into the model, we more finely resolve how a changing zooplankton community could impact FPC flux to depth. Our model results suggest that by incorporating just community size composition, estimates of zooplankton-mediated carbon flux may be improved.

The importance of copepod body size in determining FPC flux is clear, but the physical and chemical conditions that support larger- or smaller-bodied copepod communities ultimately drive interannual variability in flux. Our results show decadal changes in FPC flux. These changes are consistent with the previously documented ecosystem shift in the 1990s, when smaller copepods became more dominant and *Calanus finmarchicus* declined (Pershing et al. 2005). The decrease in modeled FPC flux and export efficiency during the late 1990s is also reflected in sediment trap data. These data document a decrease in mean annual POC export to subeuphotic depths in the Gulf between the 1990s and 2000s. Additionally, mean annual FPC flux in 1998, 2011, and 2012 stand out as the lowest in the modeled dataset. 1998 is associated with a "great salinity anomaly" (MERCINA 2012), a major oceanographic perturbation in the Gulf of Maine. The years 2011 and 2012, the final two years in our dataset, are part of a steep warming trend in the Gulf of Maine, which started in 2005. Gulf of Maine temperatures in 2012 reached record highs (Mills et al. 2013). As the North Atlantic Ocean is changing, the mean size of its copepods is decreasing (Beaugrand et al. 2010). Understanding the specific mechanisms by which physical and chemical conditions shape copepod community size structure and ecosystem state will improve understanding of variability in the copepod community, in fecal pellet carbon flux, and ultimately in the biological carbon pump.

## References


Alonso-Sáez, L., J. M. Gasol, J. Arístegui, J. C. Vilas, D. Vaqué, C. M. Duarte, and S. Agustí. 2007. Large-scale variability in surface bacterial carbon demand and growth efficiency in the subtropical northeast Atlantic Ocean. Limnol. Oceanogr. **52**: 533–546. doi: 10.4319/lo.2007.52.2.0533

Ashjian, C.J., and K.F. Wishner. 1993. Temporal and spatial changes in body size and reproductive state of Nannocalanus minor (Copepoda) females across and along the Gulf Stream. J. Plankton Res. **15**: 67–98, doi: 10.1093/plankt/15.1.67

Baltar, F., J. Aristegui, J. M. Gasol, S. Hernandez-Leon, and G. L. Herndl. 2007. Strong coast-ocean and surface-depth gradients in prokaryotic assemblage structure and activity in a coastal transition zone. Aquat. Microb. Ecol. **50**: 63–74. doi:10.3354/ame01156

Batchelder, H.P., and R. Williams. 1995. Individual-based modeling of the population dynamics of Metridia lucens in the North Atlantic. ICES J. Mar. Sci. **52**: 469–482, doi: 10.1016/1054-3139(95)80061-1

Beaugrand, G., C. Luczak, and M. Edwards. 2009. Rapid biogeographical plankton shifts in the North Atlantic Ocean. Glob. Change Biol. **15**: 1790–1803. doi:10.1111/j.1365-2486.2009.01848.x

Beaugrand, G., M. Edwards, and L. Legendre. 2010. Marine biodiversity, ecosystem functioning, and carbon cycles. Proc. Natl. Acad. Sci. USA **107**: 10120–10124. doi: 10.1073/pnas.0913855107

Behrenfeld, M. J., and E. S. Boss. 2014. Resurrecting the ecological underpinnings of ocean plankton blooms. Annu. Rev. Mar. Sci. **6**: 167–U208. doi:10.1146/annurev-marine-052913-021325

Belehrádek, J. 1935. Temperature and living matter, v. 8, 1–277. *In* Protoplasma Monograph.

Besiktepe, S., and H. G. Dam. 2002. Coupling of ingestion and defecation as a function of diet in the Calanoid copepod *Acartia tonsa*. Mar. Ecol. Prog. Ser. **229**: 151–164. doi: 10.3354/meps229151

Boyd, P. W., and P. P. Newton. 1999. Does planktonic community structure determine downward particulate organic carbon flux in different oceanic provinces? Deep-Sea Res. Pt.-I **46**: 63–91. doi:10.1016/S0967-0637(98)00066-1

Brown, J. H., J. F. Gillooly, A. P. Allen, V. M. Savage, and G. B. West. 2004. Toward a metabolic theory of ecology. Ecology **85**: 1771–1789. doi:10.1890/03-9000

Campbell, R. G., M. M. Wagner, G. J. Teegarden, C. A. Boudreau, and E. G. Durbin. 2001. Growth and development rates of the copepod *Calanus finmarchicus* reared in the laboratory. Mar. Ecol. Prog. Ser. **221**: 161–183. doi: 10.3354/meps221161

Conversi, A., S. Piontkovski, and S. Hameed. 2001. Seasonal and interannual dynamics of *Calanus finmarchicus* in the Gulf of Maine (Northeastern US shelf) with reference to the North Atlantic Oscillation. Deep-Sea Res. Pt. II **48**: 519–530. doi:10.1016/S09670645(00)00088-6

Corkett, C. J., I. A. McLaren, and J. M. Sevigny. 1986. The rearing of the marine Calanoid copepods *Calanus finmarchicus* (Gunnerus), *C. glacialis* Jaschnov and *C. hyperboreus* Krøyer with comment on the equiproportional rule. Syllogeus **58**: 539–546.

Cowles, G. W., S. J. Lentz, C. Chen, Q. Xu, and R. C. Beardsley. 2008. Comparison of observed and model-computed low frequency circulation and hydrography on the New England Shelf. J. Geophys. Res. Oceans **113**: C09015. doi:10.1029/2007JC004394

Deevey, G.B. 1960. Relative effects of temperature and food on seasonal variations in length of marine copepods in some eastern American and western European waters. Bulletin of the Bingham Oceanographic Collection **17**: 54–86.

Durbin, A. G., and E. G. Durbin. 1978. Length and weight relationships of *Acartia clausi* from Narragansett Bay. R.I. Limnol. Oceanogr. **23**: 958–969. doi:10.4319/lo.1978.23.5.0958

Feinberg, L. R., and H. G. Dam. 1998. Effects of diets on dimensions, density and sinking rates of fecal pellets of the copepod *Acartia tonsa*. Mar. Ecol. Prog. Ser. **175**: 87–96. doi:10.3354/meps175087

Folt, C. L., and C. W. Burns. 1999. Biological drivers of zooplankton patchiness. Trends Ecol. Evol. **14**: 300–305. doi:10.1016/S0169-5347(99)01616-X

Gleiber, M. R., D. K. Steinberg, and H. W. Ducklow. 2012. Time series of vertical flux of zooplankton fecal pellets on the continental shelf of the western Antarctic Peninsula. Mar. Ecol. Prog. Ser. **471**: 23–36. doi:10.3354/meps10021

Goldthwait, S. A., and D. K. Steinberg. 2008. Elevated biomass of mesozooplankton and enhanced fecal pellet flux in cyclonic and mode-water eddies in the Sargasso Sea. Deep-Sea Res. Pt. II **55**: 1360–1377. doi:10.1016/j.dsr2.2008.01.003

Greene, C. H., and A. J. Pershing. 2000. The response of *Calanus finmarchicus* populations to climate variability in the Northwest Atlantic: Basin-scale forcing associated with the North Atlantic Oscillation. ICES J. Mar. Sci. **57**: 1536–1544. doi:10.1006/jmsc.2000.0966

Guidi, L., G. A. Jackson, L. Stemmann, J. C. Miquel, M. Picheral, and G. Gorsky. 2008. Relationships between particle size distribution and flux in the mesopelagic zone. Deep-Sea Res. Pt. I **55**: 1364–1374. doi:10.1016/j.dsr.2008.05.014

Hays, G.C., P.I. Webb, and S.L. Frears. 1998. Diel changes in the carbon and nitrogen content of the copepod Metridia lucens. J. Plankton Res. **20**: 727–737, doi: 10.1093/plankt/20.4.727

Hirst, A.G., M. Sheader, and J.A. Williams. 1999. Annual pattern of Calanoid copepod abundance, prosome length and minor role in pelagic carbon flux in the Solent, UK. Mar. Ecol. Prog. Ser. **177**: 133–146, doi: 10.3354/meps177133

Hirst, A. G. 2012. Intraspecific scaling of mass to length in pelagic animals: Ontogenetic shape change and its implications. Limnol. Oceanogr. **57**: 1579–1590. doi:10.4319/lo.2012.57.5.1579

Honjo, S., and M. R. Roman. 1978. Marine copepod fecal pellets: Production, preservation and sedimentation. J. Mar. Res. **36**: 45–57.

Huntley, M. E., and M. D. G. Lopez. 1992. Temperature-dependent production of marine copepods: A global synthesis. Am. Nat. **140**: 201–242. doi: 10.1086/285410

Iversen, M. H., and L. K. Poulsen. 2007. Coprohexy, coprophagy, and coprochaly in the copepods *Calanus helgolandicus*, *Pseudocalanus elongates*, and *Oithona similis*. Mar. Ecol. Prog. Ser. **350**: 79–89. doi:10.3354/meps07095

Ji, R., C.S. Davis, C. Chen, R.C. Beardsley. 2009. Life history traits and spatiotemporal distributional patterns of copepod populations in the Gulf of Maine-Georges Bank region. Mar. Ecol. Prog. Ser. **384**: 187–205, doi: 10.3354/meps08032

Jossi, J. W., A. W. G. John, and D. Sameoto. 2003. Continuous plankton recorder sampling off the east coast of North America: History and status. Prog. Oceanogr. **58**: 313–325. doi:10.1016/j.pocean.2003.08.010

Kane, J. 2009. A comparison of two zooplankton time series data collected in the Gulf of Maine. J. Plankton Res. **31**: 249–259. doi:10.1093/plankt/fbn119

Legendre, L., and F. Rassoulzadegan. 1996. Food-web mediated export of biogenic carbon in oceans: Hydrodynamic control. Mar. Ecol. Prog. Ser. **145**: 179–193. doi:10.3354/meps145179

Litchman, E., and C. A. Klausmeier. 2008. Trait-based community ecology of phytoplankton. Annu. Rev. Ecol. Syst. **39**: 615–639. doi:10.1146/annurev.ecolsys.39.110707.173549

Litchman, E., M. D. Ohman, and T. Kiørboe. 2013. Trait-based approaches to zooplankton communities. J. Plankton Res. **35**: 473–484. doi:10.1093/plankt/fbt019

Lutz, M. J., K. Caldeira, R. B. Dunbar, and M. J. Behrenfeld. 2007. Seasonal rhythms of net primary production and particulate organic carbon flux to depth describe the efficiency of biological pump in the global ocean. J. Geophys. Res. **112**: C10011. doi:10.1029/2006JC003706

Lynch, D. R., W. C. Gentleman, D. J. McGillicuddy, and C. S. Davis. 1998. Biologicla/physical simulations of *Calanus finmarchicus* population dynamics in the Gulf of Maine. Mar. Ecol. Prog. Ser. **169**: 189–210. doi:10.3354/meps169189

Martin, J. H. 1990. Glacial-interglacial $CO_2$ change: The iron hypothesis. Paleoceanography **5**: 1–13. doi:10.1029/PA005i001p00001

Mauchline, J. 1998. The biology of Calanoid copepods. Adv. Mar. Biol. **33**: 710. doi: 10.1163/156854008784513492

McLaren, I.A. 1978. Generation lengths of some temperate marine copepods: estimation, prediction, and implications. J. Fish. Res. Board Can. **35**: 1330–1342, doi: 10.1139/f78-208

McLaren, I.A., M.J. Tremblay, C.J. Corkett, and J.C. Roff. 1989. Copepod production on the Scotian Shelf based on life-history analyses and laboratory rearings. Can. J. Fish. Aquat. Sci. **46**: 560–583, doi: 10.1139/f89-074

Melle, W., and others. 2014. The North Atlantic Ocean as habitat for *Calanus finmarchicus*: Environmental factors and life history traits. Prog. Oceanogr. **129**: 244–284. doi: 10.1016/j.pocean.2014.04.026

MERCINA. 2012. Recent Arctic climate change and its remote forcing of Northwest Atlantic Shelf ecosystems. Oceanography **25**: 208–213. doi: 10.5670/oceanog.2012.64

Mills, K. E., and others. 2013. Fisheries management in a change climate: Lessons from the 2012 ocean heat wave in the Northwest Atlantic. Oceanography **26**: 191–195. doi:10.5670/oceanog.2013.27

Møller, E. F., C. M. A. Borg, S. H. Jónasdóttir, S. Satapoomin, C. Jaspers, and T. G. Nielsen. 2011. Production and fate of copepod fecal pellets across the Southern Indian Ocean. Mar. Biol. **158**: 677–688. doi:10.1007/s00227-010-1591-5

Passow, U., and C. A. Carlson. 2012. The biological pump in a high $CO_2$ world. Mar. Ecol. Prog. Ser. **470**: 249–271. doi:10.3354/meps09985

Pasternak, A., E. Arashkevich, C. Wexels Riser, T. Ratkova, and P. Wassmann. 2000. Seasonal variation in zooplankton and suspended faecal pellets in the subarctic Norwegian Baisfjorden in 1996. Sarsia **85**: 439–452. doi:10.1080/00364827.2000.10414593

Pershing, A. J., C. H. Greene, J. W. Jossi, L. O'Brien, J. K. T. Brodziak, and B. A. Bailey. 2005. Interdecadal variability in the Gulf of Maine zooplankton community, with potential impacts on fish recruitment. ICES J. Mar. Sci. **62**: 1511–1523. doi:10.1016/j.icesjms.2005.04.025

Pilskaln, C. H., D. M. Anderson, D. J. McGillicuddy, B. A. Keafer, K. Hayashi, and K. Norton. 2014. Spatial and temporal variability of *Alexandirum* cyst fluxes in the Gulf of Maine: Relationship to seasonal particle export and resuspension. Deep-Sea Res. Pt. II **103**: 40–54. doi:10.1016/j.dsr2.2012.11.001

Primeau, F. 2005. Characterizing transport between the surface mixed layer and the ocean interior with a forward and adjoint global ocean transport model. J. Phys. Oceanogr. **35**: 545–564. doi:10.1175/JPO2699.1

Record, N. R., A. J. Pershing, and J. W. Jossi. 2010. Biodiversity as a dynamic variable in the Gulf of Maine continuous plankton recorder transect. J. Plankton Res. **32**: 1675–1684. doi:10.1093/plankt/fbq050

Record, N. R., and A. J. Pershing. 2012. First principles of copepod development help explain global marine diversity patterns. Oecologia **170**: 289–295. doi:10.1007/s00442-012-2313-0

Reygondeau, G., and G. Beaugrand. 2011. Future climate-driven shifts in distribution of *Calanus finmarchicus*. Glob. Change Biol. **17**: 756–766. doi:10.1111/j.1365-2486.2010.02310.x

Richardson, A.J., H.M. Verheye, V. Herbert, C. Rogers, and L.M. Arendse. 2001. Egg production, somatic growth and productivity of copepods in the Benguela Current system and Angola-Benguela Front. S. Afr. J. Sci. **97**: 251–257.

Richardson, A. J., and others. 2006. Using continuous plankton recorder data. Prog. Oceanogr. **68**: 27–74. doi:10.1016/j.pocean.2005.09.011

San Martin, E., R. P. Harris, and X. Irigoien. 2006. Latitudinal variation in plankton size spectra in the Atlantic Ocean. Deep-Sea Res. Pt. II **53**: 1560–1572. doi:10.1016/j.dsr2.2006.05.006

Stukel, M. R., M. D. Ohman, C. R. Benitez-Nelson, and M. R. Landry. 2013. Contributions of mesozooplankton to vertical carbon export in a coastal upwelling system. Mar. Ecol. Prog. Ser. **491**: 47–65. doi:10.3354/meps10453

Sun, X., S. Sun, C. Li, and M. Wang. 2012. Seasonal change in body length of important small copepods and relationship with environmental factors in Jiaozhou Bay, China. Chin. J. Oceanol. and Limn. **30**: 404–409, doi: 10.1007/s00343-012-1140-9

Thor, P., H. G. Dam, and D. R. Rogers. 2003. Fate of organic carbon released from decomposing copepod fecal pellets in relation to bacterial production and extracellular enzymatic activity. Aquat. Microb. Ecol. **33**: 279–288. doi:10.3354/ame033279

Tönnesson, K., T.G. Nielsen, and P. Tiselius. 2006. Feeding and production of the carnivorous copepod Paraeuchaeta norvegica in the Skagerrak. Mar. Ecol. Prog. Ser. **314**: 213–225, doi: 10.3354/meps314213

Turley, C. M., K. Lochte, and R. S. Lampitt. 1995. Transformations of biogenic particles during sedimentation in the Northeastern Atlantic. Philos. Trans. R. Soc. B **348**. doi:10.1098/rstb.1995.0060

Turner, J. T. 2002. Zooplankton fecal pellets, marine snow and sinking phytoplankton blooms. Aquat. Microb. Ecol. **27**: 57–201. doi:10.3354/ame027057

Urban-Rich, J., D. A. Hansell, and M. R. Roman. 1998. Analysis of copepod fecal pellet carbon using a high temperature combustion method. Mar. Ecol. Prog. Ser. **171**: 199–208. doi:10.3354/meps171199

Uye, S.-I. 1991. Temperature-dependent development and growth of the planktonic copepod Paracalanus sp. in the laboratory. Bulletin of Plankton Society of Japan, Special Volume, 627-636.

Uye, S., and K. Kaname. 1994. Relations between fecal pellet volume and body size for major zooplankters of the inland Sea of Japan. J. Oceanogr. **50**: 43–49. doi:10.1007/BF02233855

Uye, S., and K. Sano. 1998. Seasonal variations in biomass, growth rate and production rate of the small cyclopoid copepod *Oithona davisae* in a temperate eutrophic inlet. Mar. Ecol. Prog. Ser. **163**: 37–44. doi:10.3354/meps163037

Wanamaker, A. D., and others. 2009. A late Holocene paleoproductivity record in the western Gulf of Maine, USA, inferred from growth histories of the long-lived ocean quahog. Int. J. Earth Sci. **98**: 19–29. doi:10.1007/s00531-008-0318-z

Wexels Riser, C., P. Wassmann, K. Olli, A. Pasternak, and E. Arashkevich. 2002. Seasonal variation in production, retention and export of zooplankton faecal pellets in the marginal ice zone and central Barents Sea. J. Mar. Syst. **38**: 1175–188. doi:10.1016/S0924-7963(02)00176-8

Wexels Riser, C., M. Reigstad, and P. Wassmann. 2010. Zooplankton-mediated carbon export: A seasonal study in a northern Norwegian fjord. Mar. Biol. Res. **6**: 461–471. doi:10.1080/17451000903437067

## Acknowledgments

KS gratefully acknowledges the United States National Science Foundation Graduate Research Fellowship Program for supporting this research under grant number DGE-1144205. KS expresses thanks to J.

Runge for helpful edits. KS and AJP acknowledge further support from the United States National Science Foundation under grant number OCE-0962074. CHP acknowledges the support of NOAA grants NA04NOS4780274 and NA06NOS4780245 for the sediment trap work. NRR acknowledges support from NASA grant NNX14AM77G and Bigelow institutional funds. The authors thank four thoughtful reviewers for their comments.

*Submitted 19 November 2014*
*Revised 7 May 2015, 27 July 2015*
*Accepted 31 July 2015*

*Associate editor: Thomas Kiørboe*